Adsorption
DOI 10.1007/s10450-017-9885-2

Adsorption of laterally interacting gas mixtures on homogeneous surfaces

F. O. Sanchez-Varretti[1] · P. M. Pasinetti[2] · F. M. Bulnes[2] · A. J. Ramirez-Pastor[2]

Received: 21 December 2016 / Revised: 22 February 2017 / Accepted: 22 March 2017

Abstract The adsorption of binary mixtures containing particles A and B on homogeneous substrates is studied by Monte Carlo (MC) simulations, quasi-chemical approximation (QCA), and exact counting of states on finite cells (we call this approach cluster approximation, CA). The energies involved in the adsorption model are five: (1) ϵ_A, interaction energy between an A particle and a lattice site; (2) ϵ_B, interaction energy between a B particle and a lattice site; (3) w_{AA}, nearest-neighbor interaction energy between two A particles; (4) w_{AB} $(=w_{BA})$, nearest-neighbor interaction energy between an A particle and a B particle and (5) w_{BB} , nearest-neighbor interaction energy between two B particles. The process is monitored by following the coverage of both species with the simultaneous increasing of the individual chemical potentials of each mixture component. A non-trivial interdependence between the partial adsorption isotherms was observed and discussed in the context of the lattice-gas theory. The theoretical formalism is used to model experimental data of methane-carbon dioxide mixtures adsorbed on activated carbon. In addition, an excellent agreement was obtained between theoretical and MC simulation results. This finding evidences the usefulness of CA and QCA as a starting point to predict the behavior of a system governed by a large number of parameters.

✉ A. J. Ramirez-Pastor
antorami@unsl.edu.ar

[1] Universidad Tecnológica Nacional, Facultad Regional San Rafael, Gral. Urquiza 314, 5600 San Rafael, Mendoza, Argentina

[2] Departamento de Física, Instituto de Física Aplicada, Universidad Nacional de San Luis-CONICET, Ejército de Los Andes 950, D5700BWS San Luis, Argentina

Keywords Adsorption isotherms · Binary mixtures adsorption · Statistical thermodynamics · Monte Carlo simulations

1 Introduction

The adsorption process of gas mixtures on solid surfaces and its applications (gas separation, purification, heterogeneous catalysis, etc.) have attracted the attention of researchers for many years (Ruthven 1984; Yang 1987; Doraiswamy 1990; Smit and Maesen 2008; Dujak et al. 2015; Lauerer et al. 2015). Despite the number of contributions on this subject, the problem is far from being exhausted.

As in any adsorption process, the interactions between the adsorbed species play an important role in the mixed-gas adsorption on solids. In other words, the description of real multicomponent adsorption requires to take into account the effect of the lateral interactions in the adsorbed layer. An exact statistical mechanical treatment of this problem is unfortunately not yet available and, therefore, the theoretical description of the phenomenon relies on simplified models.

In this context, Tovbin and co-workers studied pure and mixed adsorption in the presence of lateral interactions and surface heterogeneity (Tovbin 1991, 1997; Votyakov and Tovbin 1997). By using mean-field approximation, quasi-chemical approach (QCA), and the so-called fragment cluster method, the authors investigated the main adsorption properties (isotherms and heats of adsorption), and the effects of the phase transitions occurring in the system.

Several papers from our group have focused on the study of binary gas adsorption by Monte Carlo (MC) simulation method. Simple lattice-gas models have been

Published online: 08 April 2017

investigated, and the behavior of the adsorbed phase has been studied in dependence on lateral interactions between adsorbed molecules (Bulnes et al. 2001, 2005, 2008; García et al. 2012), surface heterogeneity (Bulnes et al. 2001, 2005), and lattice geometry (Bulnes et al. 2008; García et al. 2012).

More recently, a cluster-exact approximation (CA) was presented (Sanchez-Varretti et al. 2014). This theoretical approach, based on the exact calculation of configurations on finite cells, was used to study the behavior of interacting binary mixtures adsorbed on square lattices. The CA predictions were successfully compared with MC and QCA data, demonstrating the applicability of simplified models to address a problem whose analytical treatment and experimental realization is very complex.

The results in Refs. (Bulnes et al. 2001, 2005, 2008; García et al. 2012; Sanchez-Varretti et al. 2014) are restricted to the case where the chemical potential of one species is kept constant during the adsorption process. Even though this assumption simplifies the analysis, such ideal conditions are not usually encountered in real systems. In fact, when the gas mixture is introduced directly into the reactor, the change of the total pressure in the gas phase will lead to changes in the partial pressures of the components of the gas mixture. In this line of work, Fefelov and co-workers recently studied the adsorption of a binary mixture with a simultaneous variation of the chemical potentials of both components (Fefelov et al. 2016). The effect of repulsive and attractive lateral interactions was analyzed, and a rich variety of structural orderings were observed in the adlayer.

In the case of keeping constant the chemical potential of one species, MC results have been backed up by theoretical analysis (Sanchez-Varretti et al. 2014). The same has not happened in the case studied by Fefelov and co-workers and, consequently, the results predicted by MC techniques in Ref. (Fefelov et al. 2016) have not been corroborated yet by analytical methods. The objective of this paper is to provide a thorough study in this direction.

In a previous contribution (Sanchez-Varretti et al. 2014), QCA and CA proved to be very useful tools for the research of adsorption of binary mixtures . The results showed, in addition, that the techniques could be also applied to model experimental data (Sanchez-Varretti et al. 2016). Here, the scheme introduced in Ref. (Sanchez-Varretti et al. 2014) is extended to include the analysis of binary-mixture systems with a simultaneous increasing of the chemical potentials of the mixture components. The study (i) is a natural continuation of our previous work (Sanchez-Varretti et al. 2014, 2016), (ii) complements the previous numerical analysis (Fefelov et al. 2016), and (iii) allows to test the applicability of QCA and CA in the context of the present model. The theoretical scheme is also applied to model experimental data of methane-carbon dioxide mixtures adsorbed on activated carbon.

The paper is organized in the following way. The details of the model and analytical approximations are given in Sect. 2. In Sect. 3, the MC simulation methodology is described. The results are presented and discussed in Sect. 4. Finally, the conclusions are drawn in Sect. 5.

2 Model and theory

2.1 The model

The homogeneous surface is represented by a two-dimensional square lattice of $M = L \times L$ adsorption sites with periodic boundary conditions. The substrate is exposed to an ideal A–B mixed-gas phase, at temperature T and chemical potentials μ_A and μ_B. Particles can be adsorbed on the substrate with the restriction of at most one adsorbed particle per site. Thus, this approach is limited to monolayer adsorption. In addition, nearest-neighbor (NN) interaction energies are considered.

In order to describe the system consisting of N adsorbed molecules ($N = N_A + N_B$, being $N_A[N_B]$ the number of molecules of $A[B]$ species), the occupation variable σ_i was introduced: $\sigma_i = 0$ if site i is empty, and $\sigma_i = 1[2]$ if site i is occupied by an $A[B]$ particle. The energy parameters of the model are:

(a) ϵ_A, interaction energy between a monomer type A and a lattice site.
(b) ϵ_B, interaction energy between a monomer type B and a lattice site.
(c) w_{AA}, lateral energy interaction between a NN pair A–A.
(d) w_{BB}, lateral energy interaction between a NN pair B–B.
(e) $w_{AB}(= w_{BA})$, lateral energy interaction between a NN pair A–B.

Then, in the grand canonical ensemble, the adsorbed phase is characterized by the Hamiltonian:

$$H = \frac{1}{2}\sum_{i}^{M}\sum_{l(i)}\left[w_{AA}\delta_{\sigma_i,\sigma_l,1} + w_{BB}\delta_{\sigma_i,\sigma_l,2} + w_{AB}\left(\delta_{\sigma_i,1}\delta_{\sigma_l,2} + \delta_{\sigma_i,2}\delta_{\sigma_l,1}\right)\right] + \sum_{i}^{M}\left[\epsilon_A\delta_{\sigma_i,1} + \epsilon_B\delta_{\sigma_i,2}\right] - \sum_{i}^{M}\left[\mu_A\delta_{\sigma_i,1} + \mu_B\delta_{\sigma_i,2}\right], \tag{1}$$

where the symbol δ represent the Kronecker delta, and the summation over $l(i)$ represents a sum running over the all the nearest-neighbor sites of i.

Finally, the total (θ) and partial ($\theta_{A[B]}$) surface coverage can be defined as

$$\theta = \frac{N}{M},\ \theta_{A[B]} = \frac{N_{A[B]}}{M},\ \theta = \theta_A + \theta_B. \tag{2}$$

2.2 Quasi-chemical approximation for adsorbed binary mixtures

In this section, the statistical thermodynamics of interacting binary mixtures adsorbed on homogeneous surfaces is developed on a generalization in the spirit of the lattice-gas model and the quasi-chemical approximation.

To begin, the canonical partition function corresponding to N_A and N_B particles adsorbed on a regular substrate of M sites can be written as (Hill 1960)

$$Q(N_A, N_B, M, T) = q_A^{N_A} q_B^{N_B} \sum_{N_{AA}} \sum_{N_{AB}} \sum_{N_{BB}} \Omega(N_A, N_B; N_{AA}, N_{AB}, N_{BB}; M) \times e^{-(w_{AA}N_{AA} + w_{AB}N_{AB} + w_{BB}N_{BB} + \epsilon_A N_A + \epsilon_B N_B)/k_B T} \tag{3}$$

where $q_{A[B]}$ is the partition function for a single adsorbed $A[B]$ molecule; N_{AA}, N_{AB} and N_{BB} represent the number of nearest-neighbor $A{-}A$, $A{-}B$ and $B{-}B$ pairs, respectively; $\Omega(N_A, N_B; N_{AA}, N_{AB}, N_{BB}; M)$ is the number of ways to array N_A and N_B particles on M sites with (N_{AA}, N_{AB}, N_{BB}) pairs of occupied sites; and k_B is the Boltzmann constant. The lattice allows a total number of pairs equal to $zM/2$ (z is the lattice connectivity).

As it is usual in this kind of problems, it is convenient to write the relations between N_{AA}, N_{AB}, N_{BB} and $N_{00}, N_{A[B]0}$, where N_{00} is the number of pairs of empty nearest-neighbor sites, and $N_{A[B]0}$ is the number of pairs consisting in an atom of $A[B]$ species and an adjacent empty site. Thus,

$$2N_{AA} + N_{AB} + N_{A0} = zN_A, \tag{4}$$

$$2N_{BB} + N_{AB} + N_{B0} = zN_B \tag{5}$$

and

$$2N_{00} + N_{A0} + N_{B0} = z(M - N_A - N_B). \tag{6}$$

Only three of these numbers are independent (i.e. N_{AA}, N_{AB} and N_{BB}).

By using the standard formalism of the QCA, the number of ways of assigning a total of $zM/2$ independent pairs to the six categories AA, BB, AB, $A0$, $B0$ and 00, with any number 0 through $zM/2$ per category consistent with the total, is

$$\tilde{\Omega}(N_A, N_B; N_{AA}, N_{AB}, N_{BB}, N_{A0}, N_{B0}, N_{00}; M) = \frac{\left(\frac{zM}{2}\right)!}{\left[\left(\frac{N_{A0}}{2}\right)!\right]^2 \left[\left(\frac{N_{B0}}{2}\right)!\right]^2 \left[\left(\frac{N_{AB}}{2}\right)!\right]^2 N_{AA}! N_{BB}! N_{00}!}. \tag{7}$$

By taking logarithm in Eq. (7), using the Stirling's approximation and operating, it results

$$\ln \tilde{\Omega} = \frac{zM}{2} \ln\left(\frac{zM}{2}\right) - N_{A0} \ln \frac{N_{A0}}{2} - N_{B0} \ln \frac{N_{B0}}{2} - N_{AB} \ln \frac{N_{AB}}{2} - N_{AA} \ln N_{AA} - N_{BB} \ln N_{BB} - N_{00} \ln N_{00}. \tag{8}$$

It is convenient to write $\tilde{\Omega}$ as a function of N_{AA}, N_{BB} and N_{AB}. For this purpose, we obtain N_{A0}, N_{B0} and N_{00} in terms of N_{AA}, N_{BB} and N_{AB} [using Eqs. (4–6)], and replace it in Eq. (8), then

$$\begin{aligned} \ln \tilde{\Omega}(N_A, N_B; N_{AA}, N_{BB}, N_{AB}; M) &= \frac{zM}{2} \ln\left(\frac{zM}{2}\right) - N_{AB} \ln \frac{N_{AB}}{2} - N_{AA} \ln N_{AA} - N_{BB} \ln N_{BB} \\ &- (zN_A - 2N_{AA} - N_{AB}) \ln\left[\frac{1}{2}(zN_A - 2N_{AA} - N_{AB})\right] \\ &- (zN_B - 2N_{BB} - N_{AB}) \ln\left[\frac{1}{2}(zN_B - 2N_{BB} - N_{AB})\right] \\ &- \left(\frac{zM}{2} - zN_A - zN_B + N_{AA} + N_{BB} + N_{AB}\right) \\ &\times \ln\left(\frac{zM}{2} - zN_A - zN_B + N_{AA} + N_{BB} + N_{AB}\right). \end{aligned} \tag{9}$$

$\tilde{\Omega}(N_B, N_B; N_{AA}, N_{AB}, N_{BB}; M)$ cannot be set equal to $\Omega(N_A, N_B; N_{AA}, N_{AB}, N_{BB}; M)$ in Eq. (3), because treating the pairs as independent entities leads to some unphysical configurations (see Reference (Hill 1960), p. 253). To take care of this, we must normalize $\tilde{\Omega}$:

$$\Omega(N_A, N_B; N_{AA}, N_{AB}, N_{BB}; M) = C(N_A, N_B, M)\ \tilde{\Omega}(N_B, N_B; N_{AA}, N_{AB}, N_{BB}; M), \tag{10}$$

and

$$\Omega(N_A, N_B, M) = C(N_A, N_B, M) \sum_{N_{AA}} \sum_{N_{AB}} \sum_{N_{BB}} \tilde{\Omega}(N_A, N_B; N_{AA}, N_{AB}, N_{BB}; M), \tag{11}$$

where $\Omega(N_A, N_B, M)$ is the number of ways to place N_A and N_B non-interacting particles on M sites. In the present case, this number can be exactly calculated,

$$\Omega(N_A, N_B, M) = \frac{M!}{N_A! N_B! (M - N_A - N_B)!}. \tag{12}$$

Now, as usual in the quasi-chemical formalism, $C(N_A, N_B, M)$ can be calculated using the maximum-term method (Hill 1960) in Eq. (11). The method allows us to replace $\sum_{N_{AA}} \sum_{N_{AB}} \sum_{N_{BB}} \tilde{\Omega}(N_A, N_B; N_{AA}, N_{AB}, N_{BB}; M)$ by the maximum term in the sum, $\tilde{\Omega}(N_A, N_B; N_{AA}^*, N_{AB}^*, N_{BB}^*; M)$. From the condition $\nabla \ln \tilde{\Omega}(N_{AA}, N_{AB}, N_{BB}) = 0$, we obtain

$$\begin{aligned} \frac{\partial \ln \tilde{\Omega}(N_{AA}, N_{AB}, N_{BB})}{\partial N_{AA}} &= 2 \ln\left[\frac{1}{2}(zN_A - 2N_{AA} - N_{AB})\right] - \ln N_{AA} \\ &- \ln\left(\frac{zM}{2} - zN_A - zN_B + N_{AA} + N_{AB} + N_{BB}\right) \\ &= 0, \end{aligned} \tag{13}$$

$$\frac{\partial \ln \tilde{\Omega}(N_{AA}, N_{AB}, N_{BB})}{\partial N_{BB}} = 2\ln\left[\frac{1}{2}\left(zN_B - 2N_{BB} - N_{AB}\right)\right] - \ln N_{BB} - \ln\left(\frac{zM}{2} - zN_A - zN_B + N_{AA} + N_{AB} + N_{BB}\right) = 0, \tag{14}$$

$$\frac{\partial \ln \tilde{\Omega}(N_{AA}, N_{AB}, N_{BB})}{\partial N_{AB}} = 2\ln\left[\frac{1}{2}\left(zN_A - 2N_{AA} - N_{AB}\right)\right] + 2\ln\left[\frac{1}{2}\left(zN_B - 2N_{BB} - N_{AB}\right)\right] - \frac{\ln N_{AB}}{2} - \ln\left(\frac{zM}{2} - zN_A - zN_B + N_{AA} + N_{AB} + N_{BB}\right) = 0, \tag{15}$$

and the corresponding values of N_{AA}, N_{AB} and N_{BB} giving the maximum term in the sum in Eq. (11) can be obtained by solving the equations,

$$N^*_{AA} = \frac{\left(zN_A - 2N^*_{AA} - N^*_{AB}\right)^2}{4\left(zM/2 - zN_A - zN_B + N^*_{AA} + N^*_{AB} + N^*_{BB}\right)}, \tag{16}$$

$$N^*_{BB} = \frac{\left(zN_B - 2N^*_{BB} - N^*_{AB}\right)^2}{4\left(zM/2 - zN_A - zN_B + N^*_{AA} + N^*_{AB} + N^*_{BB}\right)}, \tag{17}$$

$$N^*_{AB} = \frac{\left(zN_A - 2N^*_{AA} - N^*_{AB}\right)\left(zN_B - 2N^*_{BB} - N^*_{AB}\right)}{2\left(zM/2 - zN_A - zN_B + N^*_{AA} + N^*_{AB} + N^*_{BB}\right)}. \tag{18}$$

Then, from Eqs. (12, 16–18), and by simple algebra, $C(N_A, N_B, M)$, and consequently $\Omega(N_A, N_B; N_{AA}, N_{AB}, N_{BB}; M)$, can be calculated,

$$C(N_A, N_B, M) = \frac{\Omega(N_A, N_B, M)}{\sum_{N_{AA}}\sum_{N_{AB}}\sum_{N_{BB}}\tilde{\Omega}(N_A, N_B; N_{AA}, N_{AB}, N_{BB}; M)} = \frac{\Omega(N_A, N_B, M)}{\tilde{\Omega}(N_A, N_B; N^*_{AA}, N^*_{AB}, N^*_{BB}; M)}. \tag{19}$$

Then

$$\Omega(N_A, N_B; N_{AA}, N_{AB}, N_{BB}; M) = \frac{\Omega(N_A, N_B, M)\tilde{\Omega}(N_A, N_B; N_{AA}, N_{AB}, N_{BB}; M)}{\tilde{\Omega}(N_A, N_B; N^*_{AA}, N^*_{AB}, N^*_{BB}; M)}. \tag{20}$$

Thus, the partition function can be written as

$$Q = q_A^{N_A} q_B^{N_B} \frac{\Omega(N_A, N_B, M)}{\tilde{\Omega}(N_A, N_B; N^*_{AA}, N^*_{AB}, N^*_{BB}; M)} \sum_{N_{AA}}\sum_{N_{AB}}\sum_{N_{BB}}\tilde{\Omega}(N_A, N_B; N_{AA}, N_{AB}, N_{BB}; M) \times e^{-\left(w_{AA}N_{AA} + w_{AB}N_{AB} + w_{BB}N_{BB} + \epsilon_A N_A + \epsilon_B N_B\right)/k_B T} \tag{21}$$

The sum in (21) can be solved by applying the maximum-term method again, and replacing $\sum_{N_{AA}}\sum_{N_{AB}}\sum_{N_{BB}} C(N_A, N_B, M)\tilde{\Omega}(N_B, N_B; N_{AA}, N_{AB}, N_{BB}; M) \times \exp\left[-\left(w_{AA}N_{AA} + w_{AB}N_{AB} + w_{BB}N_{BB} + \epsilon_A N_A + \epsilon_B N_B\right)/k_B T\right]$ by the maximum term in the sum, $C(N_A, N_B, M)\tilde{\Omega}(N_B, N_B; N^{**}{}_{AA}, N^{**}{}_{AB}, N^{**}{}_{BB}; M) \times \exp\left[-\left(w_{AA}N^{**}{}_{AA} + w_{AB}N^{**}{}_{AB} + w_{BB}N^{**}{}_{BB} + \epsilon_A N_A + \epsilon_B N_B\right)/k_B T\right]$. The corresponding values of $N^{**}{}_{AA}$, $N^{**}{}_{AB}$ and $N^{**}{}_{BB}$ can be obtained by solving the equations,

$$N^{**}{}_{AA} e^{w_{AA}/k_B T} = \frac{\left(zN_A - 2N^{**}{}_{AA} - N^{**}{}_{AB}\right)^2}{4\left(zM/2 - zN_A - zN_B + N^{**}{}_{AA} + N^{**}{}_{AB} + N^{**}{}_{BB}\right)}, \tag{22}$$

$$N^{**}{}_{BB} e^{w_{BB}/k_B T} = \frac{\left(zN_B - 2N^{**}{}_{BB} - N^{**}{}_{AB}\right)^2}{4\left(zM/2 - zN_A - zN_B + N^{**}{}_{AA} + N^{**}{}_{AB} + N^{**}{}_{BB}\right)}, \tag{23}$$

$$N^{**}{}_{AB} e^{w_{AB}/k_B T} = \frac{\left(zN_A - 2N^{**}{}_{AA} - N^{**}{}_{AB}\right)\left(zN_B - 2N^{**}{}_{BB} - N^{**}{}_{AB}\right)}{2\left(zM/2 - zN_A - zN_B + N^{**}{}_{AA} + N^{**}{}_{AB} + N^{**}{}_{BB}\right)}. \tag{24}$$

Finally,

$$Q(N_A, N_B, M, T) = q_A^{N_A} q_B^{N_B} \frac{\Omega(N_A, N_B, M)\tilde{\Omega}(N_A, N_B; N^{**}{}_{AA}, N^{**}{}_{AB}, N^{**}{}_{BB}; M)}{\tilde{\Omega}(N_A, N_B; N^*_{AA}, N^*_{AB}, N^*_{BB}; M)} \times \exp\left[-\beta(\epsilon_A N_A + \epsilon_B N_B + N^{**}{}_{AA} w_{AA} + N^{**}{}_{AB} w_{AB} + N^{**}{}_{BB} w_{BB})\right]. \tag{25}$$

The chemical potential of each adsorbed species can be calculated from the free energy $F = -\ln Q$,

$$\beta\mu_{A,ads} = \left(\frac{\partial \beta F}{\partial N_A}\right)_{N_B, M, T} = \left(\frac{\partial \beta f}{\partial \theta_A}\right)_{\theta_B, T}, \tag{26}$$

and

$$\beta\mu_{B,ads} = \left(\frac{\partial \beta F}{\partial N_B}\right)_{N_A, M, T} = \left(\frac{\partial \beta f}{\partial \theta_B}\right)_{\theta_A, T}, \tag{27}$$

where $f = F/M$ and $\theta_x = xN_x/M$ $(x = A, B)$.

On the other hand, the chemical potential of each kind of molecule in an ideal gas mixture, at temperature T and pressure P, is

$$\beta\mu_{x,gas} = \beta\mu^0_x + \ln X_x P, \ \{x = A, B\}, \tag{28}$$

where X_x is the mole fraction, and μ^0_x is the standard chemical potential of the x species.

At equilibrium, the chemical potential of the adsorbed and gas phase are equal, $\mu_{x,ads} = \mu_{x,gas}$. Then,

$$\beta\mu^0_A + \ln X_A P = \left(\frac{\partial \beta f}{\partial \theta_A}\right)_{\theta_B, T}, \tag{29}$$

and

$$\beta\mu_B^0 + \ln X_B P = \left(\frac{\partial \beta f}{\partial \theta_B}\right)_{\theta_A,T}. \tag{30}$$

The theoretical procedure described in this section can be summarized as follows:

(1) Given the complete set of lateral interactions and temperature, the values of N^*_{AA}, N^*_{AB} and N^*_{BB} are obtained by solving Eqs. (16-18).
(2) Once calculated N^*_{AA}, N^*_{AB} and N^*_{BB}, $C(N_A, N_B, M)$ and $\Omega(N_A, N_B; N_{AA}, N_{AB}, N_{BB}; M)$ can be obtained (see Eqs. 19 and 20), and the partition function can be written as in Eq. (21).
(3) The partition function Q is calculated by using the maximum-term method. For this purpose, $N^{**}{}_{AA}$, $N^{**}{}_{AB}$ and $N^{**}{}_{BB}$ are obtained by solving Eqs. (22–24), and are introduced in Eq. (25).
(4) $f = -(\ln Q)/M$ is calculated, and the partial adsorption isotherms of the system are obtained from Eqs. (29) and (30).

Points 3) and 4) are numerically (and simultaneously) solved through a standard computing procedure.

2.3 Cluster approximation for adsorbed binary mixtures

Cluster approximation is based on exact calculations of configurations on a finite cell or cluster. The cluster consists of m ($m \ll M$) adsorptive sites forming a $m = l \times l$ square sub-system (in the present paper, we use $l = 4$), with adsorption energy $\epsilon_{A[B]}$ for $A[B]$ particles. As before, nearest-neighbor lateral interaction energies and periodic boundary conditions are considered. Then, the exact grand partition function for the cluster can be written as follows:

$$\Xi = 1 + \sum_{\substack{n_A, n_B = 0 \\ 1 \le n_A + n_B \le m}} {\lambda_A}^{n_A} {\lambda_B}^{n_B} \times \left\{ \sum_E g\left(E, n_A, n_B\right) \exp\left(-E/k_B T\right) \right\}, \tag{31}$$

$\lambda_A \equiv \exp\left(\mu_A/k_B T\right)[\lambda_B \equiv \exp\left(\mu_B/k_B T\right)]$ is the activity of the $A[B]$ species. $n_A[n_B]$ is the number of $A[B]$ particles adsorbed on the cluster. $g\left(E, n_A, n_B\right)$ is the number of configurations corresponding to n_A adsorbed A particles and n_B adsorbed B particles having the same energy E [see Eq. (1)],

$$E = w_{AA} n_{AA} + w_{AB} n_{AB} + w_{BB} n_{BB} + \epsilon_A n_A + \epsilon_B n_B, \tag{32}$$

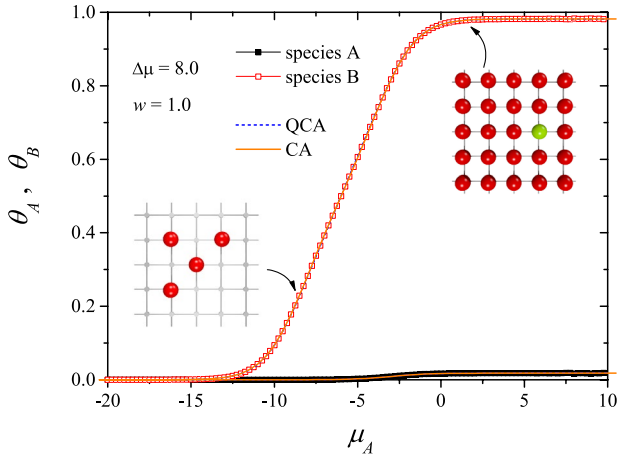

Fig. 1 Partial concentrations θ_A and θ_B as a function of $\mu_A = \mu_B - \Delta\mu$ for the case $\Delta\mu = 8$ and $w = 1$. *Symbols*, *solid lines* and *dashed lines* represent MC simulations, CA results and QCA data, respectively. Snapshots of two typical configurations of A (*green circles*) and B (*red circles*) particles are shown. The first one corresponds to the beginning of the adsorption process, whereas the second one is an example of a final configuration. (Color figure online)

where n_{AA}, n_{AB} and n_{BB} represent the number of $A-A$, $A-B$ and $B-B$ pairs, respectively, on the cluster.

The partial adsorption isotherm corresponding to the $A[B]$ species can be obtained from Eq. (31) (Hill 1960),

$$\theta_{A[B]} = \frac{k_B T}{m}\left(\frac{\partial \ln \Xi}{\partial \mu_{A[B]}}\right)_{T,\mu_{B[A]}}, \tag{33}$$

and the total coverage is $\theta = \theta_A + \theta_B$.

3 Monte Carlo simulation scheme

The adsorption of a binary mixture of gases on a homogeneous solid surface was simulated by using the grand canonical ensemble Monte Carlo method (GCMC) (Nicholson and Parsonage 1982; Rinaldi 2008).

In adsorption-desorption equilibrium there are two elementary ways to perform a change of the system state, namely, adsorbing one molecule onto the surface (adding one molecule into the adsorbed phase), and desorbing one molecule from the adsorbed phase. The corresponding transition probabilities are, respectively (Metropolis et al. 1953),

$$W_{ads}(N \to N+1) = \min\left\{1, \exp\left[-\frac{H(N+1) - H(N)}{k_B T}\right]\right\}, \tag{34}$$

and

$$W_{des}(N \to N-1) = \min\left\{1, \exp\left[-\frac{H(N-1) - H(N)}{k_B T}\right]\right\}, \tag{35}$$

where $H(N+1)-H(N)$ $[H(N-1)-H(N)]$ represents the difference between the hamiltonians of the final and initial states.

The basic algorithm to carry out an elementary Monte Carlo Step (MCS) can be summarized as follows:

(1) Set the value of μ_A, μ_B and temperature T.
(2) Set an initial state by placing randomly N molecules onto the lattice.
(3) Choose randomly one of the components of the mixture $\rightarrow X$ ($X \equiv A$ or B).
(4) Choose randomly one of the M sites, $\rightarrow i$ and generate a random number $\xi \in [0, 1]$.

(4.1) If the site i is empty, and $\xi \leq W_{ads}$, then adsorb an X particle on i. Otherwise, the transition is rejected.
(4.2) If the site i is occupied by an X particle, and $\xi \leq W_{des}$, then the X molecule is desorbed from i. Otherwise, the transition is rejected.

(5) Repeat from (3) M times.

The approximation to thermodynamic equilibrium is monitored through the fluctuations in the number N of adsorbed particles. The first $m_0 = 10^6$ MCSs are discarded in order to reach equilibrium; after that, mean values of thermodynamic quantities, like total θ and partial isotherms (θ_A and θ_B) are obtained as simple averages over $m = 10^6$ successive configurations:

$$\theta(\mu_A, \mu_B) = \frac{\langle N \rangle}{M}, \quad \theta_A(\mu_A, \mu_B) = \frac{\langle N_A \rangle}{M}, \quad \theta_B(\mu_A, \mu_B) = \frac{\langle N_B \rangle}{M}, \tag{36}$$

where the thermal average, $\langle ... \rangle$, means the time average throughout m MCSs.

The simulations were done for lattices of $l = 120$ and periodic boundary conditions in both directions. With this lattice size we verified that finite size effects are negligible.

4 Results

As discussed in Sect. 1, Fefelov et al. (Fefelov et al. 2016) studied the problem of a binary mixture with attractive AA interactions and repulsive BB interactions [each of them separately shows the classical phase transitions of first and second kind, respectively (Landau and Binder 2009; Zhdanov 1991)]. In addition, for the purity of the experiment, the authors consider that particles of different components do not interact between themselves in the model. Given the rich phenomenology exhibited by this system, the energy scheme proposed in (Fefelov et al. 2016) will be maintained in the present study. Namely, attractive inter-species lateral interaction for the A species ($w_{AA} = -w$), repulsive inter-species interaction for the B species ($w_{BB} = w$), and no interaction energy between particles of different species ($w_{AB} = 0$). We will refer to w as the (positive) magnitude of the inter-species lateral interaction.

As has already been mentioned, the restriction of the model to no more than one particle per site involves that there will be at least a excluded volume interaction between any pair of particles, no matter to what species they belong.

The case of single species adsorption, already considered previously (García et al. 2012), is reproduced here by taking $\mu_A \rightarrow -\infty$; the well-known Langmuir isotherm, passing through the point ($\mu_B/k_BT = 0$, $\theta_B = 1/2$), is obtained for $w_{BB}/k_BT = 0$. As this interaction increases and crosses a critical value, $w_c/k_BT \approx 1.763$, a plateau is developed in the isotherm at $\theta_B = 1/2$ indicating the occurrence of a $c(2 \times 2)$ ordered structure on the substrate. In the present work we can observe this effect due to the repulsive interactions between B particles.

We will consider now the adsorption and competition of the two species by varying the values of the chemical potentials μ_A/k_BT and μ_B/k_BT. The process will be monitored by measuring the amount of adsorbed particles of each species, that is, the partial and total coverage as both chemical potentials are varied simultaneously, keeping the difference $\Delta\mu = \mu_B - \mu_A$ constant. This has proved to be an interesting way of go over the (μ_A, μ_B) space to analyze the different structures that appear in the adsorbate (Fefelov et al. 2016). In addition, for the rest of the analysis we will take factor $k_BT = 1$ for simplicity and without any loss of generality, and will be omitted from the expressions.

Thus, the study was conducted in order to obtain the isotherms for different values of the lateral interaction, as well as for different values of $\Delta\mu$. The curves are shown as a function of μ_A $(= \mu_B - \Delta\mu)$.

Firstly, the value of $\Delta\mu$ was set at a small value, $\Delta\mu = 8.0$ (see Fig. 1). Then, increasing values for the magnitude of the inter-species interaction were taken, from $w = 1.0$ to 3.0.

For low chemical potential values there are no presence of any species on the substrate. When the chemical potential $\mu \approx -13$, the adsorption of the B species begins. This adsorption process starts earlier than the A species because the value of μ_B is greater than the value of μ_A. A large part of the surface is already covered by B particles at the time when the A species starts its deposition. Therefore, there are less free sites available for adsorption of A particles due to the presence of B particles.

Figures 2, 3, and 4 show, for the same $\Delta\mu$ value, the partial isotherms for increasing values of w. In the case of $w = 1.5$, the B species begins to adsorb at the same coverage than in the previous case. In this case, the greater value

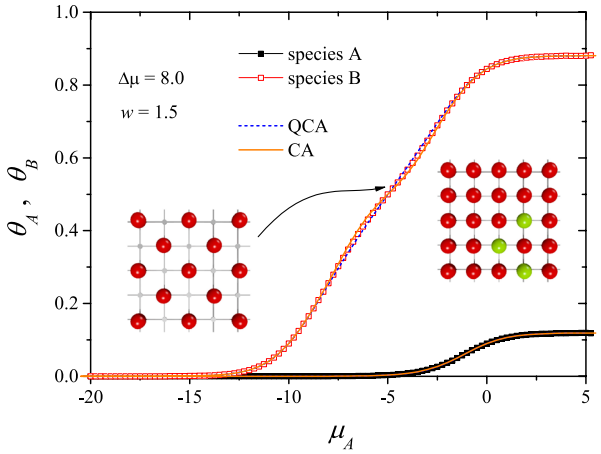

Fig. 2 Same as Fig. 1 for $w = 1.5$. Snapshots of two typical configurations of A (*green circles*) and B (*red circles*) particles are shown. The first one corresponds to the formation of the $c(2 \times 2)$ structure of B particles, whereas the second one is an example of a final configuration. (Color figure online)

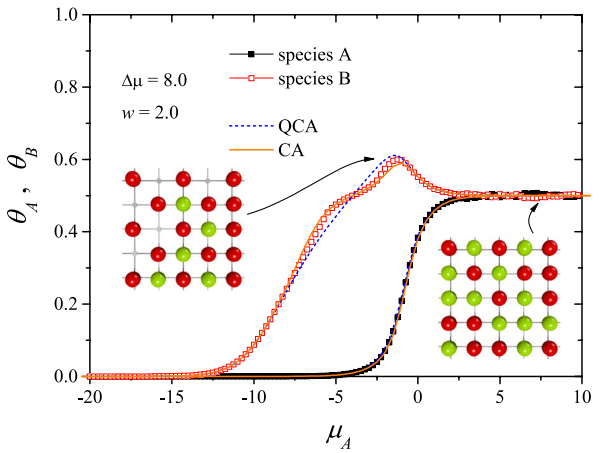

Fig. 3 Same as Fig. 1 for $w = 2$. Snapshots of two typical configurations of A (*green circles*) and B (*red circles*) particles are shown. The first one corresponds to the maximum concentration of B particles, whereas the second one is an example of a final configuration. (Color figure online)

of repulsive lateral interaction makes that the adsorbed species develops a $c(2 \times 2)$ ordered structure. Thus, it is possible to observe an incipient plateau at half coverage of the B species. This situation favors the A species to be adsorbed into the empty sites of the ordered phase. The final coverage of the A species increases, roughly of 0.1, at the expense of the coverage of the other species.

Figure 3 shows the behaviour of the system with a lateral interaction of $w = 2.0$ (and the same $\Delta\mu$ value). This case corresponds exactly to $\Delta\mu = 4w$.

The B species begins to be adsorbed at the same value as in the previous cases, but when it reaches the half coverage,

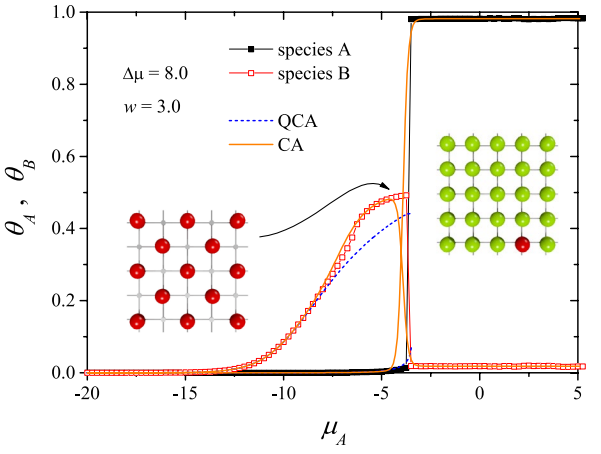

Fig. 4 Same as Fig. 1 for $w = 3$. Snapshots of two typical configurations of A (*green circles*) and B (*red circles*) particles are shown. The first one corresponds to the formation of the $c(2 \times 2)$ structure of B particles, whereas the second one is an example of a final configuration. (Color figure online)

a $c(2 \times 2)$ ordered structure is formed. Now, the deposition of A particles begins in the empty sites left by B species. As the ordered structure of B species is now more stable, A species has enough time to populate completely the empty sites. The ordered structure imposed by B species is preserved and at high chemical potentials the system have a partial coverage of ≈0.5 for both species.

In Fig. 4 we show the case of $\Delta\mu = 8$ and $w = \pm 3.0$. The adsorption of B species starts again at a chemical potential of ≈13 and rises until a coverage near 0.5.

At this point, the adsorption of A particles begins. The stronger lateral attractive interaction between A particles favors energetically the condensation of this species in the form of an abrupt jump of the isotherm. This time, the final state is the surface completely covered of A particles, displacing completely the B ones.

Now we will analyse the case were the difference between μ_A and μ_B is set to 15.0. In the Fig. 5 we can see how the surface is covered with B particles meanwhile the A particles are not adsorbed. As here the lateral energy is weak, $w = \pm 1.0$, the B particles starts up covering rapidly the surface, leaving no room for the adsorption of A particles.

The Fig. 6 shows the case of lateral interaction energy $w = \pm 2.0$ and the same value of $\Delta\mu$. The formation of a $c(2 \times 2)$ ordered structure can be observed at the partial coverage 0.5. Nevertheless, given the large $\Delta\mu$ value, B particles continue filling the surface until the total coverage, preventing the insertion of A particles. In all the range of chemical potential the coverage of the A particles is zero.

In Fig. 7 the plateau is more marked and includes a wider range of chemical potential; the lateral interaction energy is $w = \pm 3.0$. This situation allows A species to be

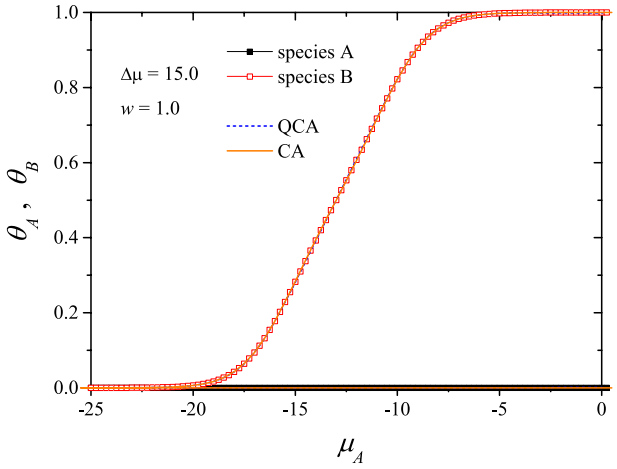

Fig. 5 Partial concentrations θ_A and θ_B as a function of $\mu_A = \mu_B - \Delta\mu$ for the case $\Delta\mu = 15$ and $w = 1$. *Symbols*, *solid lines* and *dashed lines* represent MC simulations, CA results and QCA data, respectively

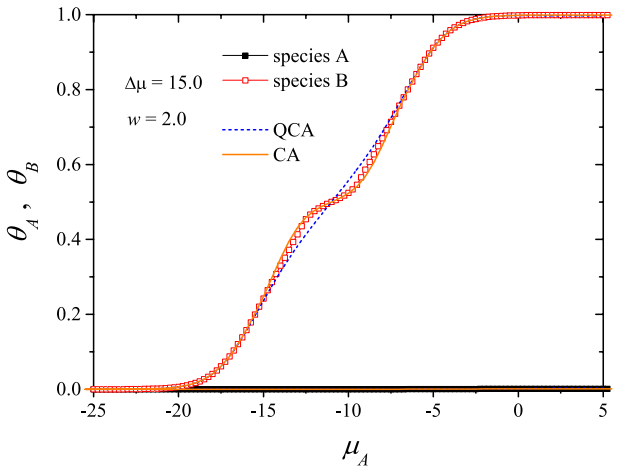

Fig. 6 Same as Fig. 5 for $w = 2$

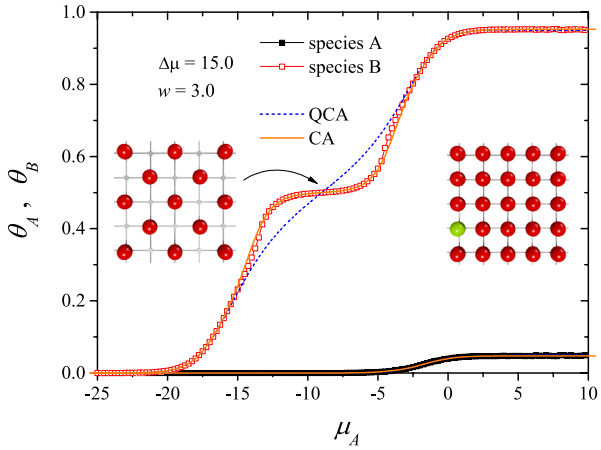

Fig. 7 Same as Fig. 5 for $w = 3$. Snapshots of two typical configurations of A (*green circles*) and B (*red circles*) particles are shown. The first one corresponds to the formation of the $c(2 \times 2)$ structure of B particles, whereas the second is an example of a final configuration. (Color figure online)

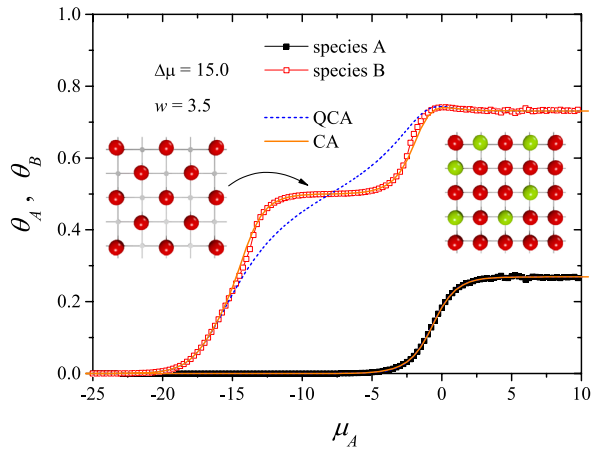

Fig. 8 Same as Fig. 5 for $w = 3.5$. Snapshots of two typical configurations of A (*green circles*) and B (*red circles*) particles are shown. The first one corresponds to the formation of a $c(2 \times 2)$ structure of B particles, whereas the second is an example of a final configuration. (Color figure online)

inserted into the surface so that there is a final non zero coverage of A particles.

The next case in Fig. 8 corresponds to a lateral interaction energy of $4w = \pm 14$, close to $\Delta\mu$. Again, the ordered structure of B particles allows the adsorption of A particles, reaching now a higher final coverage.

Figure 9 shows the formation of the ordered structure of B species followed by the insertion of additional particles of both species. The energetic cost of any additional particle is the same, given that $\Delta\mu = 4w$, nevertheless, additional B particles are rapidly replaced by A particles. This entropic competitive effect makes the final partial coverage of both species almost the same.

Increasing the lateral interaction to $w = \pm 4.0$, Fig. 10, makes the adsorbed structure of B species be partially displaced by the A species. This effect is more marked as the lateral interaction energy is greater than $\Delta\mu/4$.

In Figs. 11, 12, 13, 14, 15, 16, and 17, we show the cases corresponding to $\Delta\mu = 30$ and for interaction energies ranging from 1 to 8. A detailed analysis of each curve could be carried out by following similar arguments to those used in the analysis of previous figures. In relation to the MC results obtained in these cases, it is important to note that the unusually high magnitude used for both $\Delta\mu$ and w (remember that $k_B T$ was taken equal to unity) greatly impairs the equilibration of the MC runs (consisting on simple Metropolis steps). This limitation can be mainly

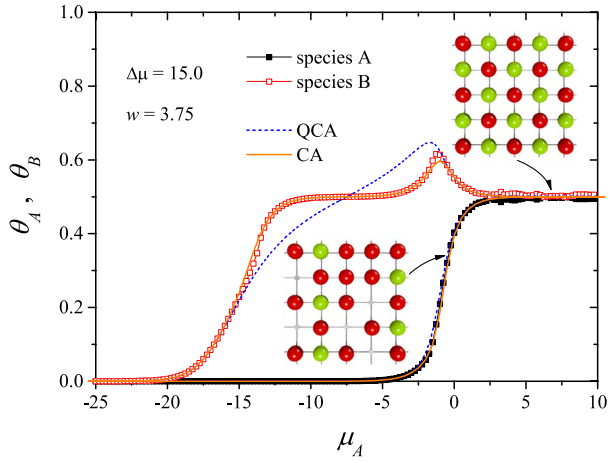

Fig. 9 Same as Fig. 5 for $w = 3.75$. Snapshots of two typical configurations of A (*green circles*) and B (*red circles*) particles are shown. The first one corresponds to the point of maximum concentration of B species, whereas the second is an example of a final configuration. (Color figure online)

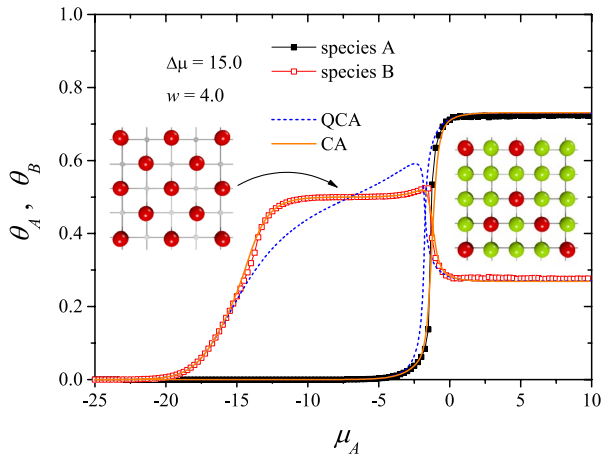

Fig. 10 Same as Fig. 5 for $w = 4$. Snapshots of two typical configurations of A (*green circles*) and B (*red circles*) particles are shown. The first one corresponds to the formation of the $c(2 \times 2)$ structure of B particles, whereas the second is an example of a final configuration. (Color figure online)

observed in the last part of the partial coverage shown in Figs. 15 and 17.

Finally, analysis of experimental results extracted from Reference (Buss 1995) has been carried out in order to test the applicability of the proposed theoretical scheme. For this purpose, experimental adsorption isotherms of pure CO_2, pure CH_4 and their binary mixtures at different fixed proportions were analyzed using the theoretical scheme presented here. Given that the experimental data were reported in adsorbed amount (moles per kg) as a function of pressure (MPa), the theoretical isotherms were rewritten in terms of pressure P [see

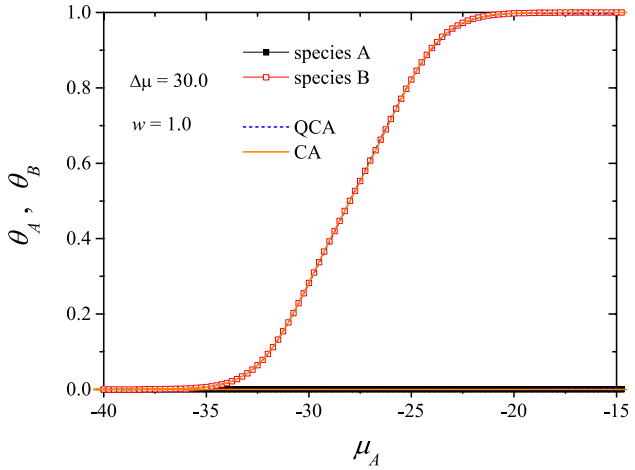

Fig. 11 Partial concentrations θ_A and θ_B as a function of $\mu_A = \mu_B - \Delta\mu$ for the case $\Delta\mu = 30$ and $w = 1$. *Symbols*, *solid lines* and *dashed lines* represent MC simulations, CA results and QCA data, respectively

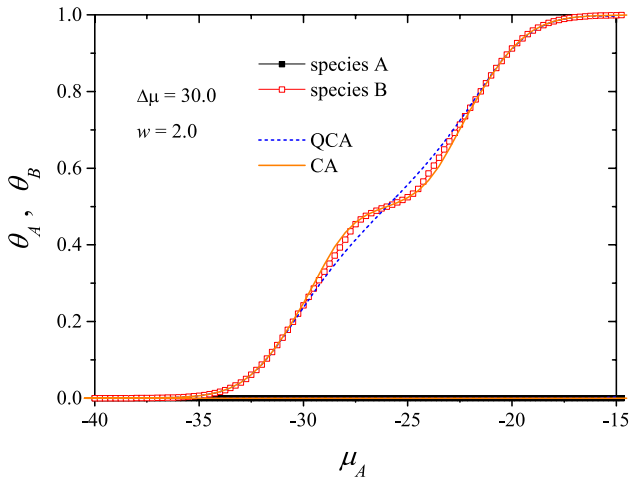

Fig. 12 Same as Fig. 11 for $w = 2$

Eq. (28)] and adsorbed amount $g = \theta g_{max}$ (being g_{max} the maximum amount of adsorbed molecules) as fitting quantities.

The substrate was modeled as a homogeneous surface. Figure 17 shows the best fit of the pure gas isotherms and their mixtures. Symbols correspond to experimental data from Reference (Buss 1995): pure methane isotherm (open circles); pure carbon dioxide isotherm (solid circles); (0.50)carbon dioxide-(0.50)methane mixture isotherm (solid squares); and (0.09)carbon dioxide-(0.91) methane mixture isotherm (open squares). Lines represent theoretical data from CA and QCA[1]. The values of

[1] Curves corresponding to QCA and CA are indistinguishable for these values of interaction energy.

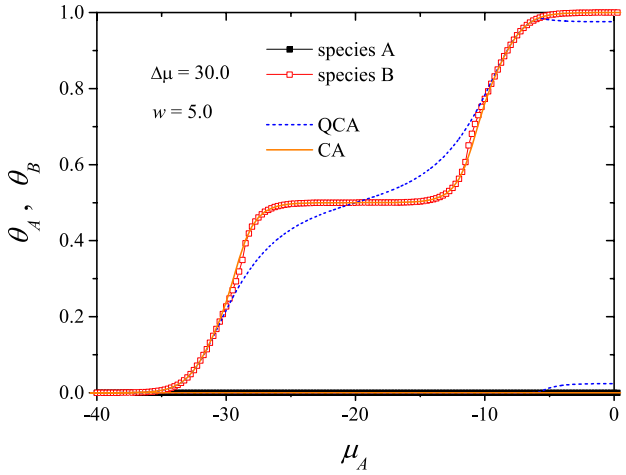

Fig. 13 Same as Fig. 11 for $w = 5$

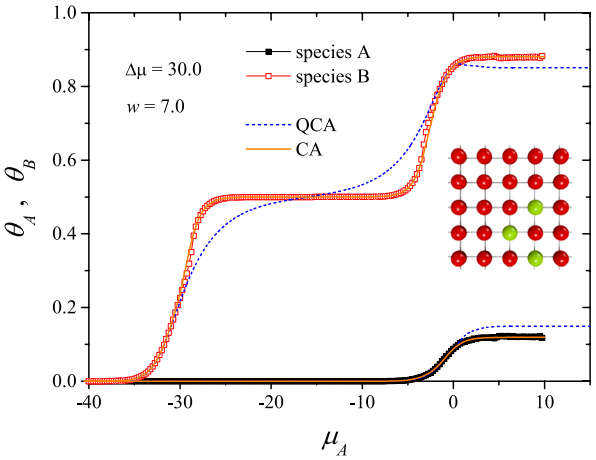

Fig. 14 Same as Fig. 11 for $w = 7$. A snapshot of typical final configuration of A (*green circles*) and B (*red circles*) particles is shown. (Color figure online)

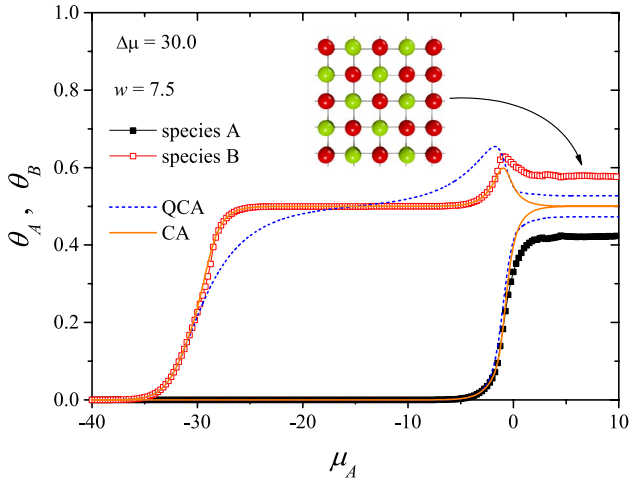

Fig. 15 Same as Fig. 11 for $w = 7.5$. A snapshot of typical final configuration of A (*green circles*) and B (*red circles*) particles is shown. (Color figure online)

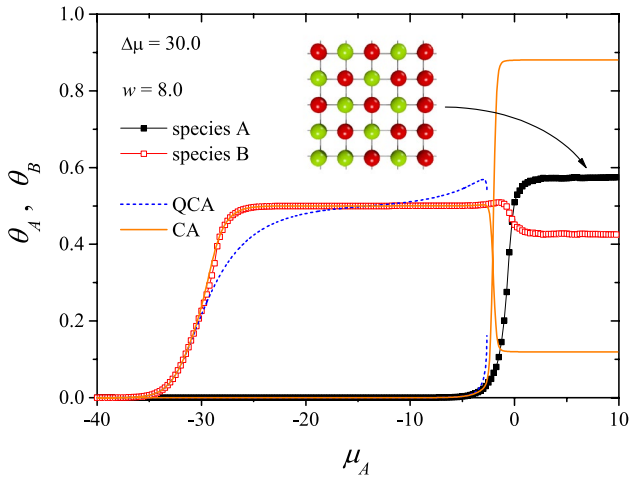

Fig. 16 Same as Fig. 11 for $w = 8$. A snapshot of typical final configuration of A (*green circles*) and B (*red circles*) particles is shown. (Color figure online)

fitting parameters are: species A (CO_2); species B (CH_4); $T = 293K$; $\Delta\epsilon = (\epsilon_B - \epsilon_A) = 0.45$ kcal/mol; $w_{AA} = -0.04$ kcal/mol; $w_{BB} = 0.05$ kcal/mol; $w_{AB} = 0$; g_{max} species A 12.19 mol/kg; and g_{max} species B 6.93 mol/kg.

As can be observed from Fig. 17, a very good agreement between experimental and theoretical data is observed. This finding shows that the theoretical scheme proposed here is a good one considering the complexity of the physical situation which is intended to be described, and could be very useful in interpreting experimental data.

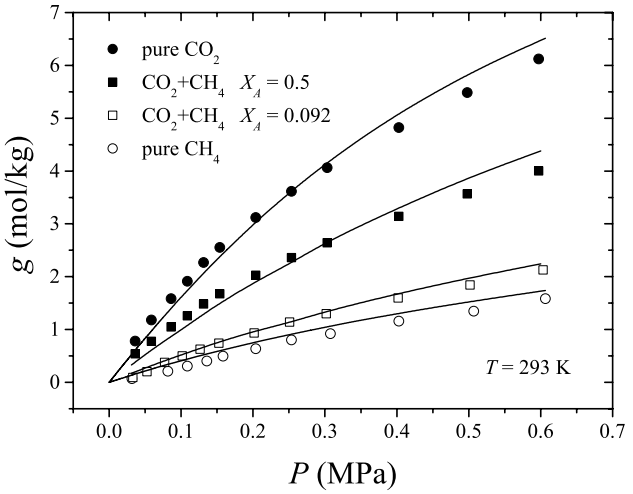

Fig. 17 Pure gas and binary mixture adsorption isotherms of carbon dioxide-methane mixtures on activated carbon at 293 K. *Symbols* correspond to experimental data from Reference (Buss 1995): pure methane isotherm (*open circles*); pure carbon dioxide isotherm (*solid circles*); (0.50)carbon dioxide-(0.50)methane mixture isotherm (*solid squares*); and (0.09)carbon dioxide-(0.91)methane mixture isotherm (*open squares*). *Lines* represent theoretical fitting curves. The fitting parameters are given in the text

5 Conclusions

In the present work, quasi-chemical approach and cluster approximation have been applied for the study of adsorption of binary mixtures with the simultaneous increasing of the individual chemical potentials of each component. The adsorption process has been monitored by following total and partial isotherms for different values of the lateral interactions between the adsorbed species. Theoretical results were complemented with Monte Carlo simulations in the grand canonical ensemble.

Following previous work in the literature (Fefelov et al. 2016), we considered here the case of $w_{AA} = -w$ (attractive interaction energy between A particles); $w_{BB} = w$ (repulsive interaction energy between B particles); and $w_{AB} = 0$ (zero interaction energy between A and B particles). In addition, the chemical potentials of both gas components were simultaneously varied, keeping the difference $\Delta\mu = \mu_B - \mu_A$ constant. A rich variety of behaviors was observed for different values of the ratio $w/\Delta\mu$.

- For $w/\Delta\mu < 1/4$, B particles begin the adsorption early than the A particles due the difference between chemical potential. At low values of μ the B species were adsorbed in all the lattice and the other type of particle can‘t be adsorbed. Finally the monolayer where covered exclusively by B particles. The $\Delta\mu$ value between both chemical potential is greater than the repulsive lateral interaction of the adsorbed particles hinder the adsorption of the A particles. A $c(2\times 2)$ structure appear in the monolayer. It happens because the lateral repulsive interaction between B particles; it makes that this particles occupy all the lattice sites with not nearest neighbour forming a chess like order in the lattice and a plateau can be observed at 0.5 of the B particles coverage. When the μ_A chemical potential is increased the A particles begin the adsorption in the empty sites of the $c(2\times 2)$ structure. Then this empty sites are covered with both type of particles until the monolayer is completed.
- For $w/\Delta\mu \simeq 1/4$, B particles begin the adsorption earlier than the A type like in the previous case and build the ordered phase $c(2\times 2)$. Here the attractive lateral interaction between A particles with 4 neighbour is of the order of $\Delta\mu$. This cause that the A specie began rapidly the adsorption in the free sites of the lattice and it facilite that newest particles adsorb in the nearest neighbour sites. The A particles occupy the $c(2\times 2)$ free structure replacing the already B adsorbed particles. This effect make that the coverage o the B particles down to 0.5. The A species have the same coverage and are embedded in the $c(2\times 2)$ structure.
- For $w/\Delta\mu > 1/4$, the B specie were adsorbed initially like in previous cases and the coverage rise to 0.5 and form the $c(2\times 2)$ structure. In that case the lateral attractive interaction is greater than $\Delta\mu$. When the A species began the adsorption its replace rapidly the B particles previously adsorbed. This effect inhibit the adsorption of B particles and the coverage of them decreases.

In general, the theoretical results present a very good qualitative and quantitative agreement with the MC data, CA being the most accurate for all cases. The agreement is excellent in the range $w/k_BT < 2$ (most of the experiments in surface science are carried out in this range of interaction energy).

Finally, the theoretical results were applied to analyze experimental data of methane-carbon dioxide mixtures adsorbed on activated carbon. The substrate was modeled as a homogeneous surface, and adsorbate-adsorbate interactions were considered. An excellent agreement between theoretical and experimental data was found. These findings demonstrate that the application of simple theoretical models, such as the QCA and CA employed in this study, can be very useful to obtain a very reasonable description of the process of adsorption of mixtures with lateral interactions.

Acknowledgements This work was supported in part by CONICET (Argentina) under Project PIP 112-201101-00615; Universidad Nacional de San Luis (Argentina) under Project 322000; Universidad

Tecnológica Nacional, Facultad Regional San Rafael (Argentina) under Project PID UTN 3542 and the National Agency of Scientific and Technological Promotion (Argentina) under Project PICT-2013-1678. S.V.F.O. would like to thank to engineer Alfredo Serra for the motivational talks with him and to the students of the degree in Business Administration for the support received.

References

Bulnes, F., Ramirez-Pastor, A.J., Pereyra, V.D.: Study of adsorption of binary mixtures on disordered substrates. J. Mol. Catal. Chem. **167**, 129 (2001)

Bulnes, F., Ramirez-Pastor, A.J., Zgrablich, G.: Monte Carlo simulation of the adsorption of binary gas mixtures on heterogeneous surfaces. Adsorpt. Sci. Technol. **23**, 81 (2005)

Buss, E.: Gravimetric measurement of binary gas adsorption equilibria of methane-carbon dioxide mixtures on activated carbon. Gas Sep. Purif. **9**, 189 (1995)

Doraiswamy, L.K.: Catalytic reactions and reactors: a surface science approach. Prog. Surf. Sci. **37**, 1 (1990)

Dujak, D., Lončarević, I., Budinski-Petković, Lj, Vrhovac, S.B., Karač, A.: Adsorption–desorption processes of polydisperse mixtures on a triangular lattice. Phys. Rev. E **91**, 032414 (2015)

Fefelov, V.F., Stishenko, P.V., Kutanov, V.M., Myshlyavtsev, A.V., Myshlyavtseva, M.D.: Monte Carlo study of adsorption of additive gas mixture. Adsorption **22**, 673 (2016)

García, G.D., Sanchez-Varretti, F.O., Bulnes, F., Ramirez-Pastor, A.J.: Monte Carlo study of binary mixtures adsorbed on square lattices. Surf. Sci. **606**, 83 (2012)

Hill, T.L.: An Introduction to Statistical Thermodynamics. Addison-Wesley Publishing Company, Reading (1960)

Landau, D.P., Binder, K.: A Guide to Monte Carlo Simulations in Statistical Physics. Cambridge University Press, Cambridge (2009)

Lauerer, A., Binder, T., Chmelik, C., Miersemann, E., Haase, J., Ruthven, D.M., Kärger, J.: Uphill diffusion and overshooting in the adsorption of binary mixtures in nanoporous solids. Nat. Commun. **6**, 7697 (2015)

Metropolis, N., Rosenbluth, A.W., Rosenbluth, N.M., Teller, A.H., Teller, E.: Equation of state calculations by fast computing machines. J. Chem. Phys. **21**, 1087 (1953)

Nicholson, D., Parsonage, N.G.: Computer Simulation and the Statistical Mechanics of Adsorption. Academic Press, London (1982)

Rinaldi, P., Bulnes, F., Ramirez-Pastor, A.J., Zgrablich, G.: Monte Carlo study of multicomponent adsorption on triangular lattices. Surf. Sci. **602**, 1783 (2008)

Ruthven, D.M.: Principles of Adsorption and Adsorption Processes. Wiley, New York (1984)

Sanchez-Varretti, F.O., Garcia, G.D., Pasinetti, P.M., Ramirez-Pastor, A.J.: Adsorption of binary mixtures on two-dimensional surfaces: theory and Monte Carlo simulations. Adsorption **20**, 855 (2014)

Sanchez-Varretti, F.O., Bulnes, F.M., Ramirez-Pastor, A.J.: A cluster-exact approximation study of the adsorption of binary mixtures on heterogeneous surfaces. Appl. Surf. Sci. **387**, 268 (2016)

Smit, B., Maesen, T.L.M.: Molecular simulations of zeolites: adsorption, diffusion, and shape selectivity. Chem. Rev. **108**, 4125 (2008)

Tovbin, Y.K.: The Theory of Physical Chemistry processes at a Gas-Solid Interfaces. Mir Publishers & CRC Press, Boca Raton (1991)

Tovbin, Y.K.: The hierarchy of adsorption models for laterally interacting molecules on heterogeneous surfaces. Langmuir **13**, 979 (1997)

Votyakov, E.V., Tovbin, Y.K.: Phase states of mixed adspecies on heterogeneous surfaces. Langmuir **13**, 1079 (1997)

Yang, R.T.: Gas Separation by Adsorption Processes. Butterworth, London (1987)

Zhdanov, V.P.: Elementary Physicochemical Processes on Solid Surfaces. Springer, Boston (1991)